

INTERMITTENCY OF FLUID IMBIBITION IN DISORDERED MEDIA

INTERMITENCIA EN "EMBEBIMIENTO" FLUIDO EN MEDIOS DESORDENADOS

X. CLOTET^{a,b}, S. SANTUCCI^{a,c}† AND J. ORTÍN^b

a) Laboratoire de Physique, CNRS UMR 5672, Ecole Normale Supérieure de Lyon, 46 Allée d'Italie, 69364 Lyon Cedex 07, France, stephane.santucci@ens-lyon.fr†

b) Departament d'Estructura i Constituents de la Matèria, Universitat de Barcelona, Martí i Franquès 1, 08028 Barcelona, Spain

c) Centre for Advanced Study at The Norwegian Academy of Science and Letters, Drammensveien 78, 0271 N-Oslo, Norway

† corresponding author

We present an experimental study of the global velocity spatially averaged over the length scale ℓ , $V_\ell(t)$, of an air-liquid interface during the forced-flow imbibition of a viscous wetting liquid in a disordered medium. Thanks to a high resolution fast camera, we have followed directly the imbibition front and observed a complex dynamics, governed by power-law distributed avalanches on a wide range of durations and sizes [1, 2]. We characterize here this intermittent behavior by studying the statistical properties of the global velocity increments $\Delta V_\ell(\tau) \equiv V_\ell(t + \tau) - V_\ell(t)$ for various time lags τ . In particular we show that the shape of the PDF of $\Delta V_\ell(\tau)$ evolve with increasing τ from fat tail exponentially stretched PDFs towards a Gaussian PDF above a characteristic time τ_c , which corresponds to the characteristic avalanche duration.

Presentamos un estudio experimental de la velocidad global promediada espacialmente a escala ℓ , $V_\ell(t)$, de una interfaz aire-líquido en "embebimiento" a flujo constante en un medio desordenado de un líquido viscoso que moja el medio. Mediante una cámara de alta resolución hemos seguido directamente el frente de "embebimiento", observando una dinámica compleja gobernada por avalanchas distribuidas en ley de potencias en un amplio rango de duraciones y tamaños [1, 2]. Caracterizamos este comportamiento intermitente estudiando las propiedades estadísticas de los incrementos de la velocidad global $\Delta V_\ell(\tau) \equiv V_\ell(t + \tau) - V_\ell(t)$, para varios intervalos de tiempo τ . En concreto mostramos que la forma de la distribución de probabilidad de $\Delta V_\ell(\tau)$, a medida que τ aumenta, evoluciona de una distribución de colas largas a una distribución Gaussiana para τ mayor que un tiempo característico, τ_c , que corresponde a la duración característica de las avalanchas.

PACS: Fluctuation phenomena statistical physics, 05.40.-a; structure and roughness of interfaces, 68.35.Ct; fluid flow through porous media, 47.56.+r; fractals fluid dynamics, 47.53.+n

INTRODUCTION

Fluid invasion in disordered media -similarly to a wide variety of slowly driven heterogenous systems such as the motion of magnetic domain walls in disordered ferromagnets [3], wetting contact lines on rough substrates [4] or crack growth in heterogenous media [5, 6], exhibits a burst-like correlated dynamics spanning a very broad range of temporal and spatial scales [7-9]. Such a complex dynamics, generically referred to as "crackling noise", is the result of several competing forces acting at different length scales: while the fluctuations in capillary forces and the heterogeneous permeability destabilize the fluid interface, viscosity and surface tension damp the resulting interfacial fluctuations, leading finally to long-range correlations along the imbibition front. The correlation length, which measures the extent of the lateral correlations, is given by $\ell_c = \sqrt{\kappa / Ca}$, where κ is the permeability of the medium, and Ca the capillary number. As a consequence, imbibition fronts in a disordered medium undergo a complex kinetic roughening process characterized by an intermittent dynamics. In the limit $Ca \rightarrow 0$ the system displays critical interfacial fluctuations [10].

More specifically, using high resolution fast imaging in quasi two-dimensional forced-flow imbibition, we have shown recently that the front motion is driven by localized avalanches, power-law distributed both in sizes and durations, with exponentially decaying cutoffs that are related to the lateral correlations of the interface and diverge as the driving velocity decreases [2]. We demonstrated that the critical spatiotemporal dynamics observed during forced-flow imbibition can be described within the framework of a pinning-depinning transition. Moreover, we have shown that these local avalanches lead to a complex temporal activity of the global advancement of the front, with in particular large global velocity fluctuations that follow an asymmetric non-Gaussian distribution with a large exponential tail, due to the presence of spatial correlations along the front and finite-size effects [1, 11].

In the present work we go further on in the investigation of the global dynamics of imbibition fronts, and quantify the global intermittent behavior. Specifically, we analyze

the statistical properties of the global velocity increments $\Delta V_\ell(\tau) \equiv V_\ell(t + \tau) - V_\ell(t)$ for various time lags τ , and we show that the PDF of $\Delta V_\ell(\tau)$ evolves with increasing τ from fat tail exponentially stretched PDFs towards a Gaussian PDF above a characteristic time τ_c , which corresponds to the characteristic avalanche duration.

EXPERIMENTAL SETUP

The setup used in the present work (Fig. 1) has been previously described in Ref. [2]. It consists on a Hele-Shaw (HS) cell of $190 \times 500 \text{ mm}^2$ (width \times length), made of two parallel thick glass plates separated by a narrow gap spacing. We introduce dichotomic fluctuations in space of the gap thickness, $b = 0.46 \text{ mm}$ and $b - \delta b = 0.40 \text{ mm}$. These spatial fluctuations are provided by copper patches of size $0.4 \times 0.4 \text{ mm}^2$ and height $\delta b = 0.06 \text{ mm}$, randomly distributed over a fiberglass substrate attached to the bottom plate and filling 35% of the total area. The patches do not overlap, and their orientation is shown in the bottom panel of Fig. 1.

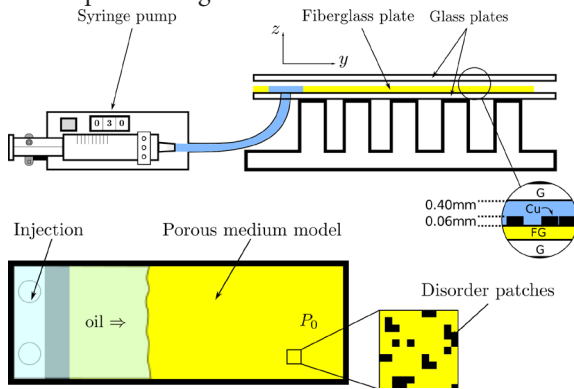


Figure 1: Sketches of the experimental setup. Top panel: the control parameter v is set by the syringe pump. The zoom on the right is a lateral view of the disordered HS cell, showing the parallel glass plates (G) and the fiberglass (FG) substrate with the copper obstacles (Cu). Bottom panel: sketch of the cell from top. The right end is open to air. The oil penetrates from the injection point at constant flow rate (constant average velocity v) and fills the porous medium model, displacing the resident fluid (air). The zoomed region shows the disorder patches and their orientation with respect to the fluid front.

We use a silicone oil (Rhodorsil 47V) as invading fluid, with dynamic viscosity $\mu = 52 \text{ mPa}\cdot\text{s}$, density $\rho = 1000 \text{ kg/m}^3$, and oil-air surface tension $\sigma = 20.7 \text{ mN/m}$ at room temperature ($23 \text{ }^\circ\text{C}$). The oil wets perfectly the glass plates, the copper patches and the fiber-glass substrate. The fluid is driven into the cell at a constant flow rate imposed by a syringe pump. Here, we will study the fluid invasion for one imposed flow rate corresponding to a mean front velocity $v = 0.131 \text{ mm/s}$. Thus, both the local front height and the local velocity are correlated along the fluid interface up to the length scale $\ell_c = \sqrt{\kappa / (\mu v / \sigma)} = 7 \text{ mm}$, that corresponds to 5% of the system size $L = 136 \text{ mm}$. We have performed 19 different experiments that explore various disorder realizations.

In the course of an experiment the interface propagates about 150 mm in the y direction before reaching a statistically stationary state with constant RMS fluctuations of the front

height. The motion of the oil-air front is then recorded using a Motion Pro X3 plus video-camera with 1280 pixels in the transverse direction and 256 to 280 pixels in the direction of fluid advancement (y). The typical spatial resolution is $r = 0.106 \text{ mm/pixel}$. We record about 10000 images per experiment at 100 fps (frames per second). An edge-tracking algorithm is applied to obtain the front position $h(x, t)$. In order to measure the local velocity $v(x, h(x, t))$ of the front we use a method developed for slow crack growth in heterogeneous materials [5], which consists on computing the waiting time $wt(x, y = h(x, t))$ that the front has spent on each position during its propagation. The local velocity map is then computed as $v(x, h(x, t)) = r/wt(x, y = h(x, t))$. Finally, from this local measurement, the global velocity of the front can be computed at any window size ℓ , as $V_\ell(t) = \frac{1}{\ell} \int_\ell v(x, t) dx$.

EXPERIMENTAL RESULTS

We will examine here the temporal fluctuations of the average velocity $V_\ell(t)$ as a function of the measuring window length scale ℓ . As shown on Fig. 3, even though the injection rate is constant, we observe that $V_\ell(t)$ is a jerky signal with a complex intermittent behavior characterized by very large positive fluctuations or avalanches [1]. We consider an avalanche as the occurrence of $V_\ell(t)$ above an arbitrary threshold, chosen here as the mean velocity $\langle V_\ell(t) \rangle$ (which would correspond to the imposed velocity v in an infinite system). We define the size S and duration T of an avalanche in the form shown in the bottom panel of Fig. 3. The avalanche size S represents the extra displacement of the average front within the duration T .

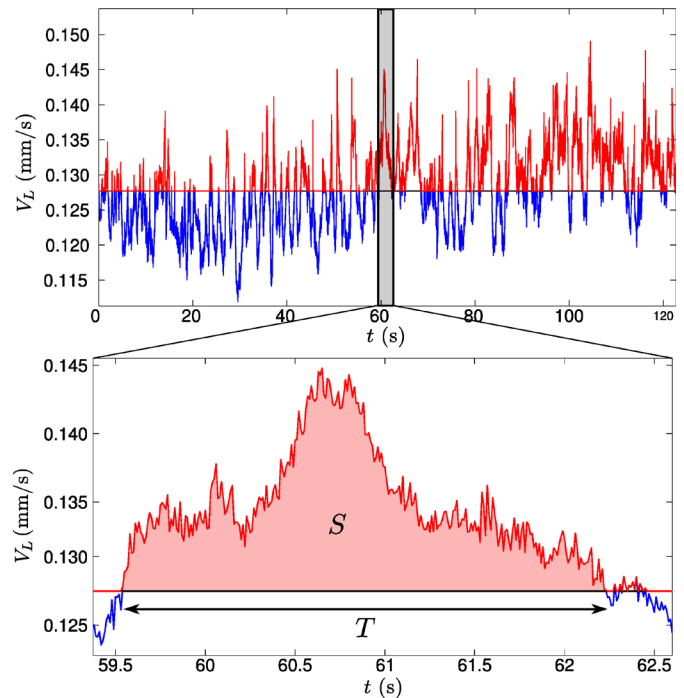


Figure 2: The top panel shows the global velocity signal for $\ell = L$, clipped by its average value. In the bottom panel a single avalanche is depicted, with size S and duration T .

We focus now on the statistics of avalanche durations in two

cases, depending on whether the global velocity V_ℓ is computed for $\ell < \ell_c$ or $\ell > \ell_c$. The corresponding distributions of avalanche durations are plotted in Fig. 3. In the top panel ($\ell > \ell_c$) we observe that the PDFs follow a power law with exponential cutoffs T_c that increase as the length of the measuring window ℓ is shortened towards ℓ_c . The inset shows the evolution of these cutoffs with ℓ . In the bottom panel ($\ell < \ell_c$), in contrast, the PDFs are exponential and do not evolve.

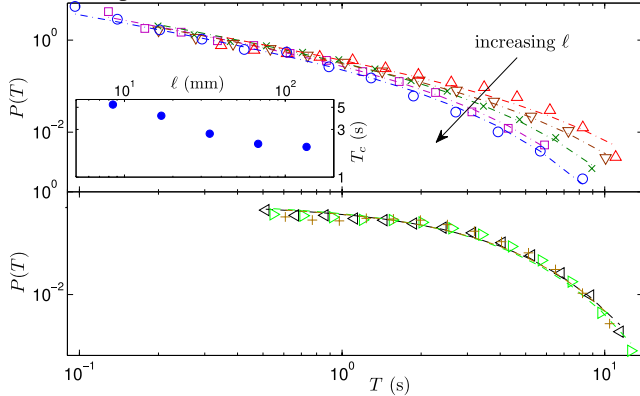


Figure 3: Top panel: PDFs of avalanche durations T , for window sizes $\ell = L/n (> \ell_c)$ with $n = 1, 2, 4, 8, 16$. Dashed lines are fits to power laws with exponential cutoffs. In the inset the cutoff duration T_c is plotted as a function of ℓ . Bottom panel: PDFs of avalanche durations T , for window sizes $\ell = L/n (< \ell_c)$ with $n = 32, 40, 50$. Dashed lines are fits to decaying exponentials with nearly the same characteristic duration $T_c = 2.06 \pm 0.06$.

In order to study the temporal fluctuations of $V_\ell(t)$, we analyze the statistical properties of the global velocity increments $\Delta V_\ell(\tau)$ for various time delays τ , and observation length scales ℓ . Such analysis has been originally proposed to study the intermittent behavior of turbulent flows [12]. We show on Fig. 4 the distributions of the normalized velocity increments $Y \equiv (\Delta V_\ell - \langle V_\ell \rangle) / \sigma_{\Delta V_\ell}$ for logarithmically increasing time lags τ and the global velocity measured at $\ell = L/8$. Interestingly, we observe that the shape of these distributions evolves through the temporal scales τ from fat tail exponentially stretched distributions at small time lags towards Gaussian distributions above a characteristic time τ_c . Such behavior is indicative of the intermittent character of the fluid invasion process, and uncovers complex temporal correlations [12-14] for durations shorter than τ_c .

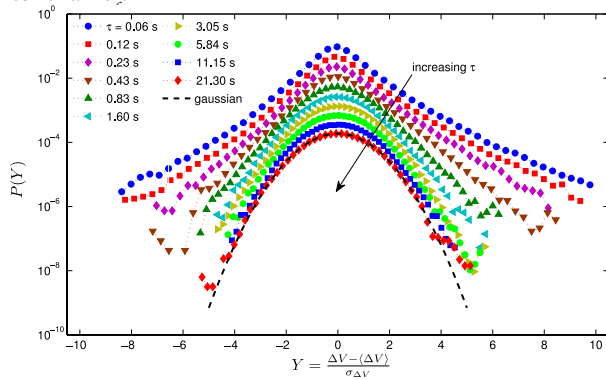


Figure 4: Semilog plot of $P(Y)$ vs $Y \equiv (\Delta V_\ell - \langle V_\ell \rangle) / \sigma_{\Delta V_\ell}$ (dotted lines) for increasing time lags τ and for $\ell = L/8$, shifted vertically for visual clarity. The PDFs evolve from fat tail distributions for $\ell < \ell_c$ to Gaussian distributions for $\tau > \tau_c \simeq 2$ s. A Gaussian PDF (dashed line) is also plotted as a guide to the eye.

To characterize and quantify the flatness of these PDFs, we compute the kurtosis $k \equiv E(x - \langle x \rangle)^4 / \sigma^4$ of the distributions $P(\Delta V_\ell(\tau))$, where E stands for the expected value. On Fig. 5 we represent the kurtosis vs. the time lag τ , varying systematically the measuring window size ℓ . We observe that the kurtosis decreases systematically as τ and ℓ increase. Above a characteristic duration τ_c it converges to the value $k_G = 3$ of a Gaussian signal whenever $\ell > \ell_c$, in agreement with the result of the previous Fig. 4. In contrast, for $\ell < \ell_c$ the kurtosis at large τ saturates to $k > k_G$, implying that the underlying statistics is not Gaussian. Below τ_c , the increase of the kurtosis at progressively shorter temporal scales seems to be close to a power law $k \propto \tau^{-\alpha}$. The power-law exponent α measures the intermittency strength of the global velocity at short durations [14]. Its evolution with the measuring window length scale is reported in the inset of Fig. 5.

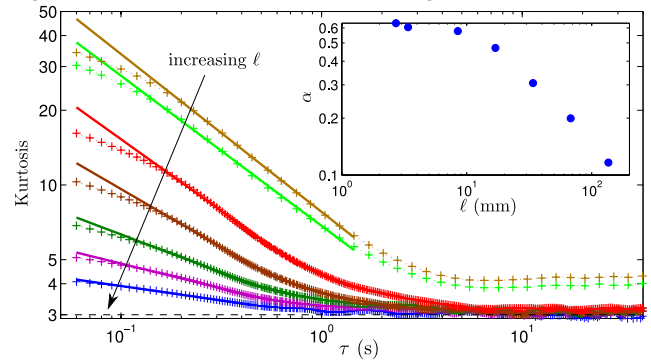


Figure 5: Kurtosis of $\Delta V_\ell(\tau)$ for $\ell = L/n$ and $n = 1, 2, 4, 8, 16, 40, 50$, in log-log scale. The kurtosis is a measure of the flatness of the distribution. The dashed line represents the value for a Gaussian distribution, $k_G = 3$. Solid lines are power-law fits, $\tau^{-\alpha}$, for small τ . Inset: exponent α as a function of ℓ .

Finally, we have extracted the characteristic time τ_c at which the kurtosis flattens out. Interestingly, the values of τ_c and especially their evolution with the measuring window size ℓ appear very close to the typical durations of the global avalanches, defined as $\langle T \rangle$. This similar trend is shown in Fig. 6.

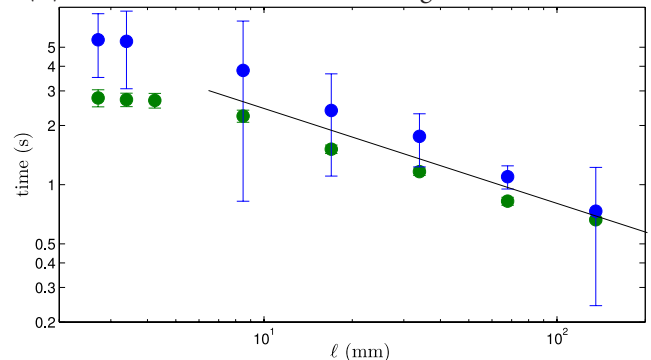


Figure 6: Characteristic times τ_c and $\langle T \rangle$ vs ℓ in log-log scale. The values of τ_c (squares) are obtained from analyzing the kurtosis of $P(\Delta V_\ell(\tau))$ with $\ell = L/n$ and $n = 1, 2, 4, 8, 16, 40, 50$. Those of $\langle T \rangle$ (circles) are the mean duration of avalanches for $\ell = L/n$ and $n = 1, 2, 4, 8, 16, 40, 50$. The solid line is plotted as a guide to the eye for $\ell > \ell_c$.

CONCLUSIONS

By analyzing the statistical behavior of the differences in the global velocity of imbibition fronts in time lapses τ and

observation windows ℓ , we have shown that the dynamics displays the characteristic features of an intermittent process. The shape of the PDF of $\Delta V_\ell(\tau)$ evolves with increasing τ from a fat tail exponentially stretched PDF to a Gaussian PDF above a characteristic time τ_c , which corresponds to the characteristic avalanche duration.

-
- [1] R. Planet, S. Santucci and J. Ortín, Phys. Rev. Lett. **102**, 94502 (2009).
 - [2] S. Santucci, R. Planet, K. Jørgen Måløy and J. Ortín., Europhys. Lett. **94**, 46005 (2011).
 - [3] G. Durin and S. Zapperi, Phys. Rev. Lett. **84**, 4705 (2000).
 - [4] E. Rolley, C. Guthmann, R. Gombrowicz and V. Repain,

Phys. Rev. Lett. **80**, 2865 (1998).

- [5] K. J. Måløy, S. Santucci, J. Schmittbuhl and R. Toussaint, Phys. Rev. Lett. **96**, 045501 (2006).
- [6] D. Bonamy, S. Santucci and L. Ponsón, Phys. Rev. Lett. **101**, 045501 (2008).
- [7] M. Kardar, Phys. Rep. **301**, 85 (1998).
- [8] D. S. Fisher, Phys. Rep. **301**, 113 (1998).
- [9] J. P. Sethna, K. A. Dahmen and C. R. Myers, Nature **410**, 242 (2001).
- [10] M. Alava, M. Dubé and M. Rost, Adv. Phys. **53**, 83 (2004).
- [11] R. Planet, S. Santucci and J. Ortín, Phys. Rev. Lett. **105**, 029402 (2010).
- [12] B. Castaing, Y. Gagne and E. J. Hopfinger, Physica D **46**, **177** (1990).
- [13] E. Bertin, Phys. Rev. Lett. **95**, 170601 (2005).
- [14] L. Chevillard, B. Castaing, A. Arneodo, E. Leveque, J. -F. Pinton and S. Roux, arXiv:1112.1036 (2011).